Adsorption and diffusion dynamics of a Ge adatom on the Si{100}(2×1) surface

Deepak Srivastava and Barbara J. Garrison
Department of Chemistry, 152 Davey Laboratory, The Pennsylvania State University, University Park, Pennsylvania 16802
(Received 20 November 1991; revised manuscript received 9 March 1992)

The Ge-adatom adsorption and diffusion on the fully relaxed Si{100}(2×1) surface is studied by a combination of molecular-dynamics simulations with Tersoff's potential for the Ge-Si interactions, a simplified transition-state theory of Voter and lattice-gas simulations. Six local minima for adsorption are found on the surface, and the activation energies between each are determined. The macroscopic diffusion follows the Arrhenius behavior with $D=4.3\times10^{-4}\exp(-0.73\ \text{eV}/kT)\ \text{cm}^2/\text{sec}$. In addition, we find that the adatom diffusion is anisotropic in nature and the direction of easy diffusion is perpendicular to the dimers (i.e., parallel to the dimer rows) of the original surface. A comparison with the Si-adatom diffusion shows that the Ge-adatom diffusion is less anisotropic and that Ge adatoms diffuse 2–3 times more slowly than Si adatoms on the same surface. The diffusion coefficients for Ge- and Si-adatom migrations perpendicular to the dimer rows are found to be $D_{\perp}^{\text{Ge}}=2.8\times10^{-3}\exp(-1.17\ \text{eV}/kT)\ \text{cm}^2/\text{sec}$ and $D_{\perp}^{\text{Si}}=4.8\times10^{-3}\exp(-1.20\ \text{eV}/kT)\ \text{cm}^2/\text{sec}$, respectively.

I. INTRODUCTION

Recent studies of Ge/Si heteroepitaxy have been stimulated by the prospect of controlling the growth of Ge/Si heterostructures at a microscopic level.[1–6] The heterostructures are generally grown in molecular-beam-epitaxy (MBE) chambers where Ge or Si atoms from an oven source are deposited onto a constant-temperature Si or Ge substrate, respectively. The typical rate of deposition (0.1 layer/min) (Ref. 7) is such that the deposited atoms migrate on the clean surface for fairly long times before coming across another atom, a surface defect, or another possible nucleation site. The diffusion of an adatom on the surface is thus important for understanding the growth processes. Although diffusion experiments have not been reported for Ge adatoms on Si{100}(2×1), analogous experiments of Si on Si{100}(2×1) (Refs. 8–10) have indicated an anisotropy in the diffusion and a possible correlation with the surface reconstruction.[11] It is expected that this anisotropy can be used in controlling the shapes of growing thin films and superlattices on the Si{100} face.[12]

Aspects of the theoretical description of the MBE growth of Si and Ge on Si{100}(2×1) have been developed. We have shown that the molecular-dynamics (MD) simulations are useful for identifying adsorption sites and mechanisms of dimer opening that lead to epitaxial growth and also interlayer diffusion.[13–16] It is noted, however, that MD simulations by themselves cannot explore the role of surface diffusion in the MBE dynamics.[17] Consequently, in a recent work, we have combined temperature-corrected simplified transition-state theory (STST) with MD and lattice-gas (LG) simulations to determine the kinetically averaged Si diffusion rates on the Si{100}(2×1) surface.[17] The computed diffusion coefficient agrees well with the recent scanning-tunneling-microscope studies of the Si/Si{100}(2×1) system.[18,19] It is noted that Si diffusion is strongly anisotropic in nature and the direction of easy Si diffusion is parallel to the dimer rows of the original surface.[17–19] In this work we use the same approach to compute Ge-adatom diffusion on the fully relaxed Si{100}(2×1) surface and compare it with the Si-adatom diffusion on the same surface.[17] To our knowledge there are no other theoretical or experimental determinations of Ge-adatom diffusion on the fully relaxed Si{100}(2×1) surface.

The combined MD-STST-LG approach[17] exploits the strengths of each technique in addressing the MBE growth of Ge on Si{100}(2×1). The initial states of the growth, such as the adsorption event, are calculated explicitly with MD simulations with Tersoff's potential for Ge-Si systems.[20] The next set of events in the real system is the diffusive motions of the adsorbed atoms. The time scale of these events is too long to be studied with direct MD simulations. A possible approach is to use TST (Refs. 21 and 22) with the same Tersoff interaction potential,[20] as used in the MD simulations,[14–16] to calculate the rate constants. The simplified version of TST is appropriate for examining the diffusion of Ge on Si for several reasons. First, the system is strongly interacting with adsorption energies of 1.5–3.0 eV. Thus there will probably not be multiple hops between sites. Second, there is the possibility of several adsorption sites, each with two to four different directions with high probability of escape. The initial goal is to examine anisotropies in the diffusion and orders of magnitude differences in the escape rates. In addition, the approximations in the empirical potentials may be more severe than the simplifications in the TST. Finally, we use lattice-gas simulations with the rate constants from STST to examine the anisotropies in the kinetically averaged diffusive motion on a macroscopic scale.

Our calculations show that the diffusion coefficient follows the Arrhenius behavior with

$$D=4.3\times10^{-4}\exp(-0.73\ \text{eV}/kT)\text{cm}^2/\text{sec}\ .$$

The diffusion is anisotropic in nature and the direction of easy diffusion is parallel to the dimer rows of the original surface. Similar to the observations in Si adatom dynamics on Si{100}(2×1),[17] we find that Ge adsorption and migration into the dimer bridge [labeled D in Fig. 1(a)] site spontaneously opens the otherwise closed dimer. As the migrating Ge adatom escapes from the D site, the dimer spontaneously closes. A quantitative comparison between Ge and Si adatom dynamics shows that the Ge-to-Si diffusion ratio is weakly dependent on temperature. At 300 K the Ge adatom diffuses three times slower than the Si adatom and at 1000 K it diffuses two times slower than the Si adatom. It is shown that the difference is partly because the Ge-adatom diffusion is less anisotropic than the Si-adatom diffusion and partly because of a mass difference between Ge and Si. The surface diffusion anisotropy in both Ge- and Si-adatom dynamics on Si{100}(2×1) is quantified by computing the diffusion coefficients perpendicular to the dimer rows of the underlying surface. We find $D_{\perp}^{\mathrm{Ge}}=2.8\times10^{-3}\exp(-1.17\ \mathrm{eV}/kT)$ cm^2/sec and $D_{\perp}^{\mathrm{Si}}=4.8\times10^{-3}\exp(-1.20\ \mathrm{eV}/kT)$ cm^2/sec. The ratio of surface diffusion anisotropy in two cases shows that at low temperature (300 K) the Ge-adatom diffusion is less anisotropic, as compared to the Si-adatom diffusion, by a factor of 5 and at high temperatures (1000 K) it is only less by a factor of 2.

In Sec. II we discuss the theoretical approach to Ge-adatom diffusion on the strongly interacting fully relaxed Si{100}(2×1) substrate. Section III contains the application to the adsorption and diffusion dynamics of a Ge adatom on the Si{100}(2×1) surface and describes the main results of this work.

II. THEORETICAL APPROACH TO Ge-ADATOM DIFFUSION ON THE Si{100}(2×1) SURFACE

The Ge-adatom dynamics on the fully relaxed Si{100}(2×1) surface constitute a strongly interacting adatom-surface system. This means that the deposited atom has a tendency to bind to the nearest local binding site and reside there for fairly long times before jumping to the neighboring site and thus moving across the surface. The time scales for many successive jumps needed to compute the macroscopic diffusion, therefore, are not accessible to the typical molecular-dynamics computer simulations.[13–16] In this work we use a combined STST, MD, and LG method to study the kinetically averaged Ge-adatom adsorption and diffusion on the Si{100}(2×1) surface.[17]

In the STST approach the diffusion of an adatom is composed of random uncorrelated hops between neighboring binding sites. It is also assumed that the time taken between hops is generally much longer than the time required to complete a hop. This approximation is reasonable since the interactions in the Ge-Si system are quite strong. Thus the total escape rate from a local binding site A is[17,21]

$$k_A^{\mathrm{STST}}=\sum_{i=1,4}\nu_{Ai}\exp(-E_{Ai}/kT)\ , \tag{1}$$

where the sum over i corresponds to the four escape directions from site A, E_{Ai} is the activation energy at 0 K for the jump in the direction i, and ν_{Ai} is the vibrational frequency for the jump Ai as given by

$$\nu_{Ai}=\prod_{j=1,3}\nu_A^j\Big/\prod_{k=1,2}\nu_i^k\ . \tag{2}$$

Here ν_A^j and ν_i^k are the real vibrational frequencies when the adatom is at the local minimum A and at the saddle point in direction i, respectively. These quantities are evaluated from the positive eigenvalues of the (3×3) force constant matrices. In Eq. (1) it is assumed that the adatom in a local binding site can escape only along two orthogonal directions. If this assumption is not made then the summation in Eq. (1) must be replaced by an integral. The validity of this assumption is discussed below.

The activation energies E_{Ai} and the vibrational frequencies ν_{Ai} for use in Eqs. (1) and (2) are computed in the following manner. The adatom is constrained in a fixed lateral position on the surface. The adatom is aimed at the surface with a velocity corresponding to the constant kinetic energy at room temperature. Using molecular dynamics the entire system is allowed to relax. The entire system is then cooled such that the total energy is minimized and simultaneously the normal force on the adatom is zero. This procedure is repeated for a grid of lateral positions within a surface unit cell and an energy profile for the Ge-adatom–Si-surface interactions is obtained. The search for stationary points corresponding to all the binding sites and the transition states is then performed by a two-dimensional Newton-Raphson root-finding method. Of note is that the cooling procedure used here brings the system to 0 K; thus, the only temperature dependence in Eq. (1) is explicitly in the Boltzmann factor. In any real system the activation energies and vibrational frequencies will also be modified by the temperature of the substrate. In an earlier work on Si-adatom diffusion we computed the first-order corrections to the harmonic rate constants and found that these corrections were small.[17] Moreover, given the uncertainties in the empirical potential used in this work, the temperature-dependent corrections to the harmonic rate constants are probably not necessary.

The last step in the calculations is to use the jump frequencies in a lattice-gas simulation to compute the long-range and long-time-scale diffusion. The idea behind the lattice-gas calculations is that the adatom always resides in one or another local binding sites. The diffusion of the adatom proceeds by randomly oriented hops between the neighboring binding sites with the probability for accepting or rejecting the jump proportional to the ratio $k_{Ai}/k_A^{\mathrm{STST}}$. The time taken to complete a jump $A\rightarrow i$ is the inverse of the total escape rate k_A^{STST} computed from Eq. (1). Thousands of randomly generated hops are made and the mean-square displacement of the adatom, $\langle\Delta r^2(t)\rangle$, is evaluated as a function of the time t. The slope of the long-time portion of this curve yields the macroscopic diffusion coefficient. These calculations are repeated at a number of different temperatures.

We note that if the adatom diffusion on the surface is

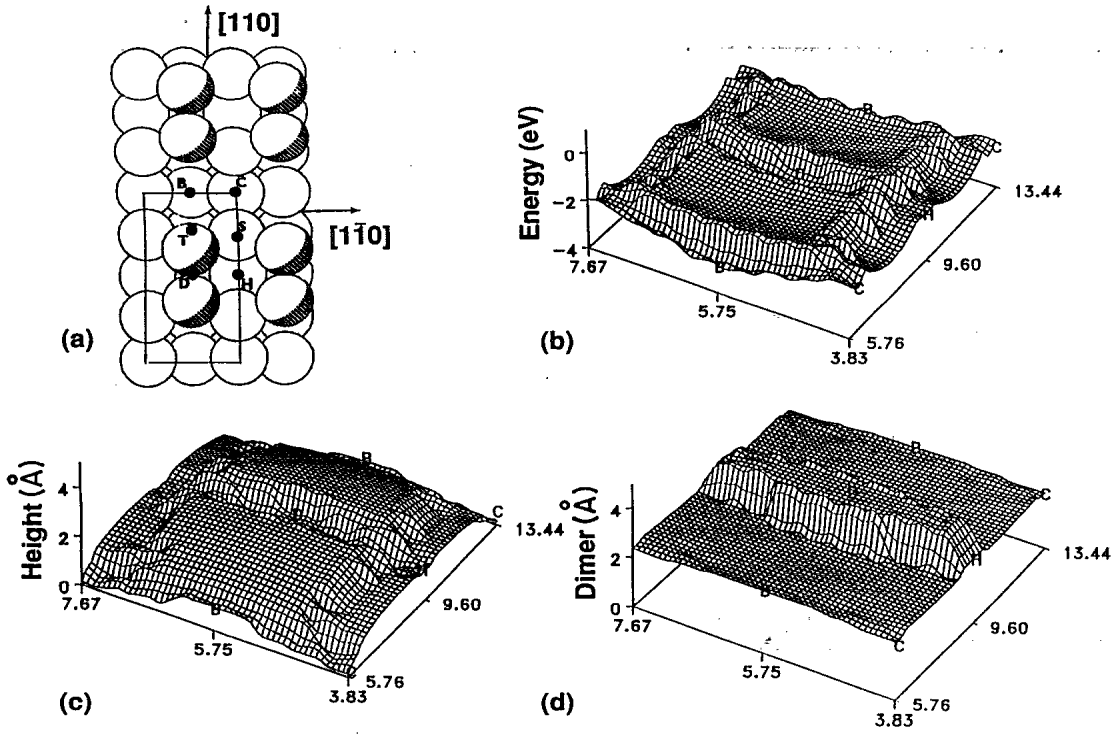

FIG. 1. Si{100}(2×1) surface. (a) (2×1) surface unit cell with unique binding sites labeled. The surface dimer atoms are shaded. (b) Energy profile for a single Ge adatom on the surface. (c) Adatom height profile above the surface plane. (d) Surface dimer bond length profile.

highly anisotropic in nature then the computed $\langle \Delta r^2(t) \rangle$, as a function of time, is predominantly composed of hops along the preferred direction of migration. Occasionally, the adatom also hops perpendicularly to the preferred direction but the statistically significant contribution of such hops is generally very small. The two independent perpendicular directions on Si{100}(2×1) surface are [1$\bar{1}$0] and [110] directions [see Fig. 1(a)]. Denoting $\Delta x(t)$ and $\Delta y(t)$ as the time-dependent displacements along the [1$\bar{1}$0] and [110] directions, respectively, we can express $\langle \Delta r^2(t) \rangle = \langle \Delta x^2(t) \rangle + \langle \Delta y^2(t) \rangle$. The mean-square displacements $\langle \Delta x^2(t) \rangle$ and $\langle \Delta y^2(t) \rangle$ can be independently computed as functions of time, and the slopes of the long-time portion of these curves will yield macroscopic diffusion coefficients along the [1$\bar{1}$0] and [110] directions, respectively. We note that the assumed separation in the dynamics along these two directions will yield independent linear curves only because in this case the diffusion is highly anisotropic, and therefore there is a natural time-scale separation in the dynamics. Of note is that statistically significant samples of displacement in a direction perpendicularly to the preferred direction of motion can only be collected by running longer-time LG "trajectories" at high temperatures.

III. COMPUTATIONS AND RESULTS

The simulation system for calculating the energies and frequencies consisted of a five-layer-thick Si slab with eight atoms per layer [Fig. 1(a)]. The bottom layer was held fixed and the remaining atoms and the Si adatom were allowed to move in the MD simulations. We have chosen to use the Tersoff potential[20] for the Ge-Si energetics to be consistent with our previous MD simulations on the adsorption process and the dimer opening mechanisms.[13–16] To obtain the adatom–surface-interaction energy profile the adatom was aimed at the surface with a velocity corresponding to 0.026 eV. The entire system, with the adatom constrained to move only normal to the surface plane, was allowed to relax for 1.5 psec (1 psec$=10^{-12}$ sec). The entire system was then slowly cooled (3–5 psec) during which time each component of the velocity of each atom was independently set to zero as it passed through a maximum value. As the entire system cooled to near 0 K the total energy of the system minimized simultaneously with the normal force on the adatom going to zero. The procedure was repeated for a grid of lateral positions within a surface unit cell. The initial grid spacing was 0.24 Å. For refinement of the minima and the transition-state locations a grid spacing as small as 0.04 Å was used. The energies are reported relative to the fully relaxed adsorbate-free Si{100}(2×1) surface. Six unique local minima are observed and their energetics and geometries are given in Table I. In addition, the energy, the adatom height above the surface plane, and the surface dimer length profiles as a function of the surface position are shown in Figs. 1(b), 1(c), and 1(d), respectively. The convergence of the results was checked at all the binding sites with respect to the variations in

TABLE I. Energetics and dynamics of Ge-adatom adsorption on the Si{100}(2×1) surface.

Site	Binding energy (eV)	Adatom height (Å)[a]	Dimer length (Å)[b]	Adsorption probability[c]	Adsorption probability[d]
$B(2,4,2)$	−2.91	1.41	2.50	0.03	0.08
$D(2,4,2)$	−2.70	1.72	3.64	0.10	0.13
$S(2,1,2)$	−2.59	1.75	2.38	0.16	0.27
$T(1,2,4)$	−2.12	2.37	2.38	0.70	0.45
$H(4,2,1)$	−2.16	1.67	2.52	0.01	0.05
$C(4,2,2)$	−1.93	0.58	2.35	0.00	0.02

[a]The adatom height is relative to the position of the surface atoms in a clean relaxed Si{100}(2×1) surface.
[b]The length of this surface dimer on the fully relaxed clean surface is 2.37 Å.
[c]The adsorption probabilities were computed in a molecular-dynamics simulation of 200 trajectories of approximately 6 psec each in duration.
[d]The adsorption probabilities estimated from the relative area of the site on the surface.

MD times for the incoming adatom (1–3 psec) and the simulation temperature of the substrate (300–1000 K) atoms. The results reported here remain converged to within 1%. The values at the energy minima were also checked with a larger crystal of 18 atoms/layer and were found to be converged to within 5% with no alterations in the qualitative features in the contour plots.

The six local minima are identified by a letter and the number of nearest-neighbor atoms of the adatom in the (surface,second,third) layers of the substrate. The long bridge $B(2,4,2)$ and the dimer bridge $D(2,4,2)$ sites are above the fourth-layer Si atoms. The cave $C(4,2,2)$ and the hollow $H(4,2,1)$ sites are over the third-layer Si atoms. The two other possible binding sites are the on-top sites over the bulk-terminated first-layer atom, $T(1,2,4)$, and over the second layer atom, $S(2,1,2)$. The T site has also been described as the dangling bond or radical site.

A. Energetics and dynamics of a Ge-adatom adsorption on the clean Si{100}(2×1) surface

The energetic and structural information in Table I and Figs. 1(b), 1(c), and 1(d) highlight several interesting features of the Ge-adatom interaction with the Si{100}(2×1) surface. First, the global minimum for the surface occurs at site B ($E=-2.91$ eV). However, this site has a very narrow region of the surface over which it occurs and it also corresponds to adsorption very close to the surface. The adsorption site T, although higher in energy, interacts with the incoming adatom while it is farthest from the surface and has a large region into which incoming atoms can be funneled. [Adsorption site T is the large plateau or mesa region of Fig. 1(b) and 1(c).] These qualitative features of the energy profiles would indicate that the direct adsorption into site T would be more probable than adsorption into site B. We computed these probabilities by simulating MD trajectories of adatom sticking on a clean surface at 0 K and also estimated the relative area of each site on the surface. As seen in Table I, adsorption into sites T, S, or D occurs in over 90% of the events. The estimated adsorption probabilities from the relative surface area are of the same order as those from MD simulations of adsorption trajectories. We also note that the results in Table I are consistent with our previous MD simulations performed using the Tersoff Ge-Si potential[20] where the dominant adsorption mechanism was into the dangling bond site.[13,16]

We note that the energy profile shown in Fig. 1(b) is qualitatively similar to the one reported for Si-adatom adsorption on the Si{100}(2×1) surface; however, at all the binding sites in Figs. 1(a) and 1(b) the Ge adatom binds less strongly to the Si surface as compared with the binding of the Si adatom on the same surface.[17] The difference in the binding energies between Si and Ge adsorption is maximum (0.56 eV) when the adatom is at the D site and minimum (0.30 eV) when the adatom is at the H site. We note that significant differences in the binding energies of Ge and Si adatoms on the Si{100}(2×1) surface, however, does not mean that the diffusion rates in the two cases will also be significantly different. The diffusion rates are determined from the activation barriers for escaping from a binding site, and we shall see later that the activation barriers for escape from most of the sites in the two cases are not much different. In Fig. 1(d) we show the length of surface dimer bond as the adatom is adsorbed and moved across the surface unit cell. The dimer length profile shows quite dramatically that substrate relaxation or rearrangement is critical when considering diffusion of adatoms in a strongly interacting system. For all sites except D the surface dimer is close. However, for the adatom directly above the surface dimer, the dimer spontaneously opens. Adsorption trajectories of this type had been previously observed in MD simulations[14–16] but, as indicated in Table I, these are not as probable as adsorption into the dangling-bond (T) site.

B. Rate constants for elementary diffusion jumps

The contour plot of the surface energetics presents a preview of the nature of the diffusion process but does not definitively describe the diffusion rates. To determine these we have also calculated the activation barriers between each of the sites. From Fig. 1(b), we note that the

TABLE II. The Ge-adatom diffusion dynamics on Si{100}(2×1) surface at 600 K.

Jump type	Activation energy (eV)[a]	Vibrational frequency (sec^{-1})[a]	Total escape rates (sec^{-1})[b]	Jump probabilities[b]
$B \rightarrow T$	1.21	0.25×10^{13}	3.98×10^{3}	0.043
$B \rightarrow C$	1.05	0.12×10^{13}		0.457
$D \rightarrow T$	0.90	0.18×10^{13}	3.94×10^{6}	0.013
$D \rightarrow H$	0.73	0.26×10^{13}		0.487
$S \rightarrow C$	0.86	0.14×10^{13}	7.48×10^{7}	0.001
$S \rightarrow T$	0.71	0.51×10^{13}		0.074
$S \rightarrow H$	0.53	0.18×10^{13}		0.851
$H \rightarrow S$	0.11	0.20×10^{13}	5.93×10^{11}	0.401
$H \rightarrow D$	0.20	0.28×10^{13}		0.099
$T \rightarrow S$	0.31	0.15×10^{13}	8.51×10^{9}	0.438
$T \rightarrow D$	0.33	0.05×10^{13}		0.099
$T \rightarrow B$	0.42	0.07×10^{13}		0.025
$C \rightarrow B$	0.06	0.10×10^{13}	6.64×10^{11}	0.471
$C \rightarrow S$	0.21	0.11×10^{13}		0.029

[a]Computed on the 0-K potential surface.
[b]Computed from Eq. (1).

minimum activation barriers from all the labeled sites are generally along the two orthogonal directions; thus, using a sum over only four directions in Eq. (1) is justified. The activation barriers and jump frequencies, therefore, as calculated by Eqs. (1) and (2) are given in Table II. The activation barriers vary from 0.06 eV ($C \rightarrow B$) to 1.21 eV ($B \rightarrow T$). These are large differences given that this energy is used in the Boltzmann factor. The vibrational frequencies, on the other hand, are used as prefactors and thus the values of $(0.05-0.51)\times10^{13}$ sec^{-1} are nearly constant. Using the activation energies and vibrational frequencies in Eq. (1) the total escape rates k_A^{STST} can be calculated. These values for a temperature of 600 K are given in Table II.

The escape rates from the various sites as given in Table II vary from 10^3 to 10^{11} jumps/sec. Correspondingly the residence times vary from milliseconds to subpicoseconds. Naturally the longest residence time is for site B, the most stable site. However, even in this site the adatom has sufficient time to diffuse during MBE growth that is occurring at the rate of 0.1–1 layer/min.[8] In addition to the overall escape rates, Table II also has the individual jump probabilities. For example, the total escape rate from site T is 8.51×10^{9} sec^{-1}. Of the total hops, 10% of the time the adatom moves into site D, 3% into site B, and 44% into each of the two equivalent adjacent S sites. Of note is that for Si-adatom diffusion, the most probable direction of escape from the T site was to the D site, whereas here it is into the S sites. Since the Ge-adatom adsorption occurs primarily in T, S, and D sites (Table I), the most probable jumps which contribute significantly to the diffusion are $T \leftrightarrow S$, $S \leftrightarrow H$, and $H \leftrightarrow D$, and the less probable jumps at the T and S sites are $T \rightarrow B$ and $S \rightarrow C$, respectively. These jump characteristics have two significant implications. First, the adsorbed Ge adatom on a dimer row most likely will remain on the same dimer row, and the second is that the adatom motion on the same dimer row will consist of almost equal visits to S, D, T, and H sites. Thus the overall anisotropy in the Ge-adatom dynamics, i.e., mainly the migration parallel to the dimer row, is the same as was the case of Si adatom diffusion.[17] The microscopic nature of the Ge-adatom motion on the same dimer row, however, is significantly different from the Si-adatom behavior on the same surface. The Ge-adatom motion has greater sideways fluctuations from the $H \leftrightarrow D$ path.

C. Lattice-gas simulations for the diffusion

The relative escape rates and jump frequencies from the various sites are useful for estimating the dominant path of diffusion but, as mentioned above, diffusion out of even the B site can occur during the MBE growth event. Lattice-gas simulations allow one to obtain a better idea of the actual diffusive processes. Correspondingly, LG simulations were performed at temperatures of 300, 600, 800, and 1000 K for the escape rates as calculated by Eq. (1). At each temperature we ran 1500 "trajectories" (random walk weighted by calculated jump probabilities) to calculate macroscopic diffusion constants. Of these we randomly picked 20 trajectories at 600 K and analyzed them, in detail, for microscopic mechanisms of adatom migration. In Fig. 2 two sample trajectories of migration are shown. Each dot represents a hop into that particular site. In about 14 out of 20 randomly chosen trajectories, that lasted up to 40 μsec, the adatom followed a path similar to that shown in trajectory 1. For the most part the adatom remains on the dimer row, migrating between S, H, D, and T sites. The second trajectory depicted in Fig. 2 shows the behavior in the remaining six trajectories in which the adatom occasionally diffuses into the trough between two dimer rows, diffuses among B and C sites, and then eventually makes it to the adjacent dimer row. Although this type of motion is less probable

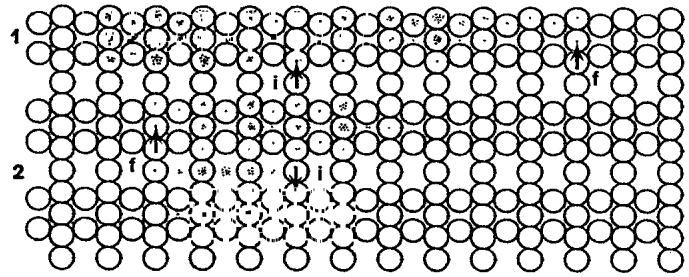

FIG. 2. Two sample trajectories of macroscopic migration. The arrows indicate the initial and the final positions of the migrating adatom and each dot in a trajectory represents a hop into that particular site. The labels *i* and *f* indicate the initial and final positions, respectively.

as diffusion along only one dimer row, we note that it can easily occur on the time scale of the MBE growth.[8] Of note is that the LG calculations demonstrate quite clearly that the overall diffusion is anisotropic, it is parallel to the dimer rows, and the adatom mainly migrates on top of the dimer row. The microscopic mechanism of the adatom jumping between two dimers on the same row shows that almost all the *S*, *H*, *D*, and *T* sites are visited equally during the jump (see, for example, most of trajectory 1). This is in contrast with the microscopic details of Si-adatom migration on the same surface where predominantly only *D* and *H* sites are visited.[17] A qualitative comparison of the analyzed trajectories with a similar analysis in Si/Si{100}(2×1) (Ref. 17) case shows that Ge diffusion is less anisotropic. For the Ge diffusion 30% of the 20 random trajectories showed the adatom hopping from one dimer row to another, whereas for the Si diffusion only 5% of the 20 random trajectories showed such behavior.[17]

The LG calculations, in addition to the mechanism of diffusion, yield the macroscopic diffusion coefficient. The diffusion coefficients at four temperatures are plotted in Arrhenius form in Fig. 3. The best-fit straight line to the

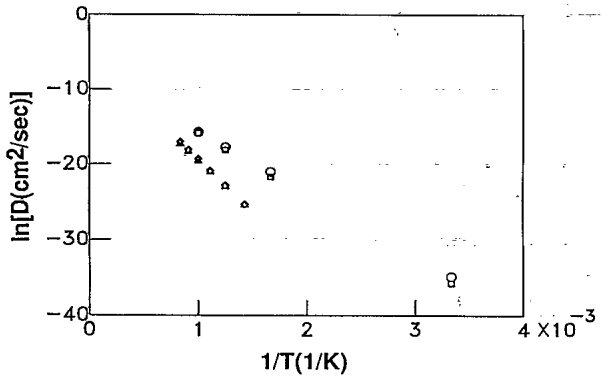

FIG. 3. Logarithm of Ge- and Si-adatom diffusion coefficients as functions of inverse temperature. The squares are for Ge-adatom diffusion and the Si-adatom diffusion values are represented by circles. The diffusion coefficients for migration perpendicular to the dimer rows are also shown. The triangles correspond to the perpendicular migration of Ge adatoms, whereas the diamonds are for Si adatoms.

TABLE III. Ratio of Ge vs Si diffusion on Si{100}(2×1).

T (K)	D_{Si} (cm²/sec)	D_{Ge} (cm²/sec)	D_{Ge}/D_{Si}	A_{Ge}/A_{Si}
300	5.46×10^{-16}	2.21×10^{-16}	0.40	4.6
600	6.27×10^{-10}	3.09×10^{-10}	0.49	2.1
800	2.05×10^{-8}	1.06×10^{-8}	0.52	1.8
1000	1.66×10^{-7}	8.85×10^{-8}	0.53	1.6

Ge data yields that the Arrhenius behavior for the self-diffusion of Ge on Si{100}(2×1) follows $D_{Ge}=4.3\times10^{4}\exp(-0.73\ \text{eV}/kT)$ cm²/sec. For comparison in Fig. 3 we have also shown the Si-adatom diffusion coefficients at the same temperatures as for the Ge-adatom diffusion.[23] The best-fit straight line to the Si data yields $D_{Si}=7.2\times10^{-4}\exp(-0.72\ \text{eV}/kT)$ cm²/sec.[17,23] In Table III we give the Ge-to-Si diffusion ratios at different temperatures. The Ge adatom diffuses two to three times slower than the Si adatom and there is a very weak temperature dependence in the ratio. The weak temperature dependence in the ratio is explained by noting that the kinetically averaged activation barrier to the Ge diffusion is only 0.01 eV larger than that for Si-adatom diffusion.[17] At low temperatures the difference in the Ge- and Si-adatom diffusion is decided by the difference in the activation barrier heights; however, as the temperature is increased the difference in the diffusion is dominated by the difference in the preexponential factors. Since the difference in the preexponential factors is implicitly dependent on the vibration frequencies (and hence on the masses) in two cases, we note that the high temperature difference in the diffusion behavior is primarily due to the mass difference between Ge and Si.

It is important to bear in mind that this calculation has been for a single adatom on a perfect surface. In addition, there is a basic assumption that the adatom remains the adatom. In a previous simulation of the growth process, mechanisms where the adatom exchanged with a surface atom were observed.[13,14] Again, this assumption can be removed, but a separate calculation must be performed.

D. Quantification of surface diffusion anisotropy

In the preceding section we have done a qualitative comparison between Ge- and Si-adatom migration behavior by analyzing 20 randomly selected LG trajectories for microscopic and macroscopic characteristics. We find that in both cases diffusion is strongly anisotropic in nature with fast diffusion parallel to and on the dimer rows of the underlying surface. The local dynamics of a Ge adatom includes almost equal visits to *S*, *D*, *H*, and *T* sites, whereas a Si adatom predominantly visits only *D* and *H* sites during the diffusion. We also find that Ge-adatom diffusion is less anisotropic as compared to the diffusion of a Si adatom on the same surface. Even

though detailed examination of LG trajectories gives us a qualitative difference between Ge- and Si-adatom diffusion, the quantitative values of the diffusion coefficients for migration perpendicular to the dimer rows of the original surface need to be computed. We do this by running LG trajectories at higher temperatures and for longer time durations. This is because, in both Ge- and Si-adatom dynamics on Si{100}(2×1), diffusion is highly favored for migration parallel to the dimer rows. At low temperatures (300–600 K) and in short-time-duration (≤ 1 μsec) trajectories, no statistically significant migration perpendicular to the dimer rows is observed. By going to a higher temperature range (700–1200 K) and running longer time (≤ 5 msec) trajectories we see statistically significant migration perpendicular to the dimer rows. The diffusion coefficients for migration perpendicular to the dimer rows, for both Ge- and Si-adatom dynamics on Si{100}(2×1), are calculated as explained above and shown in Fig. 3. The best-fit straight lines to the perpendicular diffusion data for Ge and Si yield $D_{\perp}^{\mathrm{Ge}}=2.77\times10^{-3}\exp(-1.17\ \mathrm{eV}/kT)$ cm^2/sec and $D_{\perp}^{\mathrm{Si}}=4.82\times10^{-3}\ \exp(-1.20\ \mathrm{eV}/kT)$ cm^2/sec, respectively. Defining surface diffusion anisotropy as the ratio $A=D_{\perp}/D$ between the perpendicular diffusion coefficient and the overall diffusion coefficient, we find $A_{\mathrm{Ge}}=6.51\times\exp(-0.44\ \mathrm{eV}/kT)$ and $A_{\mathrm{Si}}=6.67\times\exp(-0.48\ \mathrm{eV}/kT)$. From these values, we note that even at 1000 K both $D_{\perp}^{\mathrm{Ge}}$ and $D_{\perp}^{\mathrm{Si}}$ are about two orders of magnitude smaller than the overall diffusion coefficients. Therefore it is reasonable to assume that even at 1000 K about 95% of the overall diffusion is due to the migration parallel to the dimer rows. The relative anisotropy in Ge- and Si-adatom migration can be compared by computing the ratio $A_{\mathrm{Ge}}/A_{\mathrm{Si}}$ at different temperatures. The ratios of $A_{\mathrm{Ge}}/A_{\mathrm{Si}}$ from 300 to 1000 K are listed in Table III. At low temperatures (300 K), we find the perpendicular migration in Ge dynamics is about five times more probable than that in Si-adatom dynamics. At high temperatures (1000 K), the Ge-adatom perpendicular migration is more probable only by a factor of 2.

IV. SUMMARY

Lattice-gas simulations of a Ge-adatom diffusion on the fully relaxed Si{100}(2×1) surface have been performed. The site-to-site jump frequencies for all possible elementary diffusion hops between many local binding sites were obtained from a combination of molecular-dynamics simulations and simplified transition state theory. We find that there are six unique local binding sites on the surface. The global minimum is at the bridge site B in the trough between two dimers. However, the most probable adsorption site of a Ge atom from the gas phase is into the dangling bond or T site.

The macroscopic diffusion process is calculated to follow the Arrhenius form $D=4.3\times10^{-4}\exp(-0.73\ \mathrm{eV}/kT)$ cm^2/sec. Our calculations show that the diffusion is anisotropic with the direction of motion being parallel to the dimer rows on the underlying surface. A comparison with the Si-adatom diffusion on the same surface shows that Ge diffuses 2–3 times slower than Si on the same surface. We have found a weak temperature dependence in the Ge-to-Si diffusion ratio, indicating that the difference in the kinetically averaged activation barriers to the diffusion in the two cases is fairly small. The high-temperature behavior of the diffusion ratio is attributed to the mass difference between Ge and Si. We have quantified the anisotropy in surface diffusion for both Ge- and Si-adatom dynamics by computing the diffusion coefficients for migration perpendicular to the dimer rows of the original surface. We find that $D_{\perp}^{\mathrm{Ge}}=2.8\times10^{-3}\exp(-1.17\ \mathrm{eV}/kT)$ cm^2/sec and $D_{\perp}^{\mathrm{Si}}=4.8\times10^{-3}\exp(-1.20\ \mathrm{eV}/kT)$ cm^2/sec. The surface diffusion anisotropy as a function of temperature shows that Ge-adatom diffusion is less anisotropic as compared to that of Si-adatom diffusion.

ACKNOWLEDGMENTS

We gratefully thank the Office of Naval Research and the National Science Foundation for financial support. The Pennsylvania State University supplied a generous grant of computer time for this work.

[1]E. Kasper, H. J. Herzog, and H. Kimble, Appl. Phys. **8**, 199 (1975).
[2]J. C. Bean, Phys. Today **39** (10), 36 (1986).
[3]R. People, IEEE J. Quantum Electron **QE-22**, 1696 (1986).
[4]T. P. Pearsell, J. Bevk, L. C. Feldman, J. M. Boner, J. P. Mannaerts, and A. Ourmazd, Phys. Rev. Lett. **58**, 729 (1987).
[5]F. K. Legoues, M. Copel, and R. M. Tromp, Phys. Rev. B **42**, 11 690 (1990).
[6]D. E. Jesson, S. J. Pennycook, and J.-M. Baribeau, Phys. Rev. Lett. **66**, 750 (1991).
[7]H.-J. Gossmann and L. C. Feldman, Phys. Rev. B **32**, 6 (1985).
[8]R. J. Hamers, U. K. Köhler, and J. E. Demuth, Ultramicroscopy **31**, 10 (1989).
[9]M. G. Lagally, R. Kariotis, B. S. Swartzentruber, and Y. W. Mo, Ultramicroscopy **31**, 87 (1989).
[10]A. J. Hoeven, J. M. Lenssinck, D. Dijkkamp, E. J. Van Loenen, and J. Dieleman, Phys. Rev. Lett. **63**, 1830 (1989).
[11](2×1) symmetric dimer reconstruction on Si{100} surface; see, for example, I. P. Batra, Phys. Rev. B **41**, 5048 (1990) and references therein.
[12]See, for example, M. Tsuchiya, P. M. Petroff, and L. A. Coldren, Appl. Phys. Lett. **54**, 1690 (1989), and references therein.
[13]D. W. Brenner and B. J. Garrison, Surf. Sci. **198**, 151 (1988).
[14]D. Srivastava, B. J. Garrison, and D. W. Brenner, Phys. Rev. Lett. **63**, 302 (1989).
[15]D. Srivastava and B. J. Garrison, J. Vac. Sci. Technol. A **8**, 3506 (1990).
[16]D. Srivastava, B. J. Garrison, and D. W. Brenner, Langmuir **7**, 683 (1991).
[17]D. Srivastava and B. J. Garrison, J. Chem. Phys. **95**, 6885 (1991).

[18]Y.-W. Mo, R. Kariotis, B. S. Swartzentruber, M. B. Webb, and M. G. Lagally, J. Vac. Sci. Technol. A **8**, 201 (1990).
[19]Y.-W. Mo, J. Kleiner, M. B. Webb, and M. G. Lagally, Phys. Rev. Lett. **66**, 1998 (1991).
[20]J. Tersoff, Phys. Rev. B **39**, 5566 (1989).
[21]A. F. Voter and J. D. Doll, J. Chem. Phys. **82**, 80 (1985).
[22]A. F. Voter, Phys. Rev. B **34**, 6819 (1986).
[23]Note that Si-adatom diffusion coefficients are computed on the 0-K interaction energy profile as shown for Ge in Fig. 1(b). The first-order temperature-corrected values are reported in Ref. 17.